ASSEMBLY PROPERTIES OF GOLD NANODISCS MODIFIED WITH ALKYNE AND AZIDE LIGANDS

Melda Taspika*

Department of Physics, Faculty of Science and Technology, Universitas Islam Negeri Sulthan Thaha Saifuddin Jambi, Indonesia

Received: 8th July 2026; Revised: 30th October 2026; Accepted: 30th October 2026

ABSTRACT

Plasmonic nanoparticle assemblies have attracted considerable interest for applications in biosensing, optical devices, and biomedicine. Understanding the driving forces governing nanoparticle assembly is essential for controlling their structural and functional properties. Ligands play a critical role in regulating the assembly behavior of gold nanoparticles (AuNPs). In this study, gold nanodiscs (AuNDs) were functionalized with alkanethiol ligands via a ligand-exchange reaction, as indicated by changes in their zeta potentials before and after functionalization. The assembly behavior of AuNDs was strongly dependent on the ligand composition at their surfaces. AuNDs functionalized with thermoresponsive (**C1**) and carboxyl-functionalized (**COOH**) ligands exhibited reversible assembly and disassembly upon heating and cooling, respectively, as monitored by extinction spectroscopy. The incorporation of alkyne (**Alk**) or azide ($\mathbf{N_3}$) ligands altered the assembly and disassembly temperatures, potentially owing to differences in ligand hydrophobicity. Because alkyne and azide groups can undergo copper(I)-catalyzed azide–alkyne cycloaddition (CuAAC), this functionalization strategy may provide a basis for developing covalently linked AuND assemblies with enhanced structural stability.

Keywords: Gold Nanodiscs; Assembly; Plasmonic Nanoparticle; Alkyne; Azide

Introduction

Gold nanoparticles (AuNPs) exhibit localized surface plasmon resonance (LSPR), which arises from the collective oscillation of conduction electrons in response to incident electromagnetic radiation.[1–4] Their plasmonic properties depend on particle size, shape, and the surrounding dielectric environment.[5–7] Gold nanodiscs (AuNDs), with their anisotropic geometry and extended planar surfaces, offer a useful model for investigating how particle morphology and surface functionalization affect interparticle interactions and assembly behavior. The optical response of AuNDs is also sensitive to their dimensions, size distribution, and structural uniformity.[8]

The assembly of gold nanoparticles is governed by interparticle interactions that depend on surface ligands, solvent conditions, temperature, and particle geometry.[9,10] Surface-bound ligands stabilize nanoparticles in dispersion and can regulate the balance of attractive and repulsive interactions between particles. Alkanethiols, commonly represented as HS-$(CH_2)_n$-X, are widely used for gold surface functionalization because of the strong affinity of sulfur-containing groups for gold. The terminal functional group, X, can be selected to modify the chemical properties of the nanoparticle surface and influence interparticle interactions.[11] Thermoresponsive ligands containing hexa(ethylene glycol) segments have been employed to control the reversible assembly and disassembly of gold nanoparticles through temperature-dependent changes in ligand hydration and interparticle interactions.[12–15] The alkyl chain and terminal-group chemistry may also affect the interparticle interactions that govern the temperature-dependent assembly and disassembly of gold nanoparticles.

In parallel, click-reactive functional groups, particularly azide and alkyne, have been incorporated into gold nanostructures for covalent conjugation and nanoparticle

*Corresponding author.
E-Mail: meldataspika@uinjambi.ac.id

assembly. Previous studies have demonstrated the use of azide- and alkyne-functionalized gold nanorods and other gold nanoparticle architectures for click-mediated coupling.[16–19] These studies demonstrate that click-reactive functionalities can be incorporated into gold nanostructures for subsequent covalent conjugation. However, their role in thermally induced nanoparticle assembly remains a separate question.

Previous research on thermoresponsive AuNDs modified with **C1**- and **COOH**-terminated ligands reported hysteretic assembly–disassembly behavior and suggested that interparticle interactions, potentially involving van der Waals forces and hydrogen bonding under the investigated conditions, contribute to this behavior.[12] Such findings suggest that ligand chemistry can influence the thermal response of AuND assemblies. Although thermoresponsive assembly of AuNDs has been investigated, a direct comparison of the thermoresponsive assembly behavior of AuNDs functionalized with azide- and alkyne-terminated ligands has not been reported.[12,16–19] A direct comparison of AuNDs functionalized with alkyne- or azide-terminated ligands could help establish whether these two functionalities are associated with differences in assembly and disassembly behavior during heating and cooling. This question is relevant because the presence of click-reactive groups provides potential sites for subsequent covalent coupling, while their effects on thermally induced assembly need to be evaluated independently.

In this study, we compare the thermoresponsive assembly and disassembly behavior of AuNDs functionalized with hexa(ethylene glycol)-based ligands bearing alkyne (**Alk**) or azide (**N3**) terminal groups during heating and cooling. This comparison aims to determine whether the two ligand functionalizations are associated with differences in the temperature-dependent assembly response and its reversibility. The potential use of these complementary click-reactive groups for future CuAAC-mediated covalent coupling is also noted, although such reactions are beyond the scope of this study.

Methods

a. Materials

The **COOH** ligand was bought from Dojindo Laboratories Co., Ltd. (Japan). Thermo-responsive ligand (**C1**) and surface ligands with **Alkyne** and **N3** head were prepared in our laboratory. Sodium iodide (NaI), hydrogen tetrachloroaurate (III) trihydrate ($HAuCl_4 \cdot 3H_2O$), ascorbic acid ($C_6H_8O_6$), tris(2-carboxyethyl) phosphine hydrochloride (TCEP), sodium borohydride ($NaBH_4$), and hexadecyl trimethylammonium bromide (CTAB) were obtained from Sigma Aldrich Chemie (Germany). Sodium hydroxide (NaOH, 1 mol/L) and HEPES were purchased from Wako Pure Chemical Industries (Japan). All commercial reagents were used without further purification. All solutions were prepared with ultrapure water (Milli-Q reference system).

b. Instruments for Characterizations

UV-Vis-NIR spectrophotometers with automatic position cell changer (JASCO Corp.) was used to record the extinction spectra. For temperature-dependent measurements, 1 °C/min of heating rate and 5 min of waiting time were applied upon heating and cooling. Scanning Transmission Electron Microscopy (STEM) images were captured under 200 kV accelerating voltage of HD-2000 (Hitachi High-Tech). Observation objects were prepared by depositing 5 µL of colloidal solution onto a copper TEM-grid and dried at room temperature. Zeta potentials were measured by ZetaSizer Nano ZS (Malvern Panalytical Ltd.).

c. Preparation of Gold Nanodiscs

AuNDs were prepared by selective etching of gold nanotriangles (AuNTs) via a comproportionation reaction, as previously reported.[12] The seed solution was prepared by mixing 0.5 mL of 20 mM $HAuCl_4 \cdot 3H_2O$ with 36.5 mL of water, followed by the addition of 1 mL of 10 mM sodium citrate and 1 mL of ice-cold 100 mM $NaBH_4$ under vigorous stirring for 2 min at room temperature. The solution was incubated at 30 °C for 4 or 6 h.

For AuNT growth, 54 µL of 0.1 M NaI was added to 108 mL of 0.05 M CTAB. The solution was divided into bottles A (9 mL), B (9 mL),

This work is licensed under a Creative Commons Attribution-NonCommercial-ShareAlike 4.0 International License

and C (80 mL). $HAuCl_4 \cdot 3H_2O$, NaOH, and citric acid were added to bottles A and B (125, 50, and 50 µL, respectively; concentrations of 20, 100, and 100 mM) and bottle C (1.25, 0.5, and 0.5 mL, respectively; the same concentrations). Subsequently, 1 mL of seed solution was added to bottle A, followed by sequential transfer of 1 mL from bottle A to bottle B and the entire contents of bottle B to bottle C. These steps were performed as rapidly as possible, with a target transfer interval of approximately 5 s to promote uniform AuNT formation. Transfer times exceeding 5 s could affect seed homogeneity and the uniformity of the resulting AuNTs. After incubation at 30 °C for 24 h, the resulting AuNTs were dispersed in 20 mL of 25 mM CTAB.

AuNDs were obtained by selectively etching AuNTs through a comproportionation reaction. Briefly, 20 µL of 10 mM $HAuCl_4 \cdot 3H_2O$ was added to 5 mL of the AuNT dispersion under vigorous vortex mixing for 60 s. The mixture was incubated at 30 °C for 13 h. The reaction was terminated by removing the supernatant through two centrifugation cycles (9400 × g, 8 min, 30 °C). The resulting AuNDs were redispersed in 5 mL of 10 mM CTAB and stored at 30 °C for subsequent experiments.

d. Modifying AuNDs with Ligands

Prior to modification, ligands (**C1**, **Alk**, and **N3**) were reduced with TCEP at 30 °C for 1 h. Then, 1 mL of colloidal AuNDs was centrifuged (9,400 g, 8 min, 30 ºC) to remove excess CTAB. Next, 900 µL of supernatant was discarded before changing the solution to 700 µL of H_2O. After that, 100 µL of 2 mM CTAB and 100 µL of 5 mM concentrated ligands (**C1**, **COOH**, **Alk**, and **N3**) were added into 800 µL of AuNDs solution, followed by mixing with vortex before incubation at 30 °C for 15 hours to promote ligand exchange reaction. The second step modification was conducted with the same ligand concentration and incubated at 30 °C for 24 hours. Next, the modified AuNDs were respectively washed with 10 mM HEPES buffer (pH 8.0) and 10 mM NaOH. After centrifugation, 900 µL supernatant was removed and the same volume of HEPES or NaOH was added to the precipitated AuNDs. Then, AuNDs were continuously washed by HEPES with the same procedure twice to completely remove the excess ligands. Finally, AuNDs were dispersed in HEPES and stored at 4 °C before characterization.

Result and Discussion

a. Preparation of Gold Nanodiscs

AuNTs were synthesized using a seed-mediated method to obtain thin gold nanotriangles. However, this method has limitations, including low reproducibility, low yield, and sensitivity to the timing of seed addition, which can affect particle size and shape uniformity.[20] The extinction spectrum of AuNTs synthesized using a longer time interval (>5 s) between additions (**Figure 2a**) exhibited a broad spectral feature, suggesting a relatively broad distribution of particle properties.[21] A weak feature was also observed at approximately 1050 nm, which may be associated with the localized surface plasmon resonance (LSPR) of AuNTs. The STEM image (**Figure 2c**) showed that many particles deviated from the ideal triangular morphology, suggesting a low yield of well-defined triangular particles. Reducing the time interval between additions improved the apparent uniformity of the resulting AuNTs, as observed in the STEM image (**Figure 2d**). This observation was accompanied by a sharper extinction peak centered at 1215 nm (**Figure 2b**), suggesting a narrower distribution of optical responses. Nevertheless, the spectral sharpening and morphological observations should be considered complementary evidence, as the LSPR peak position and linewidth can also depend on particle size, shape, and aspect ratio.

This work is licensed under a Creative Commons Attribution-NonCommercial-ShareAlike 4.0 International License

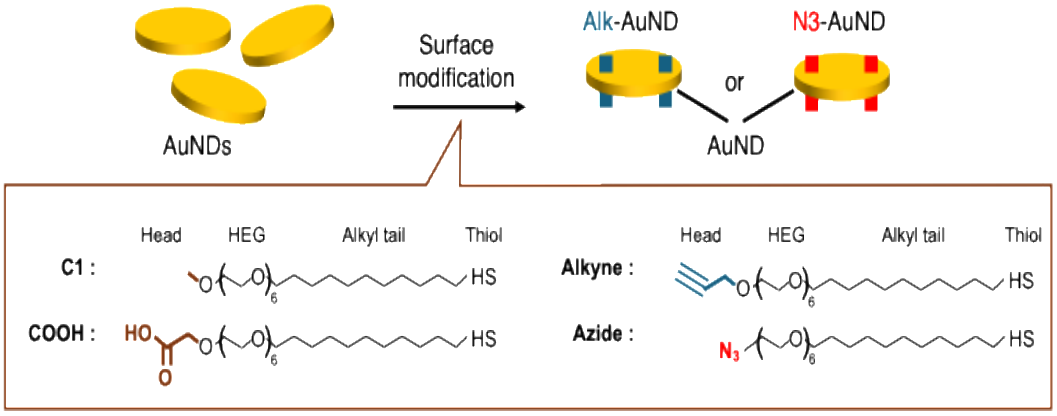


Figure 1. Surface modification of AuNDs with Alkyne (**Alk**) and Azide (**N3**) ligand

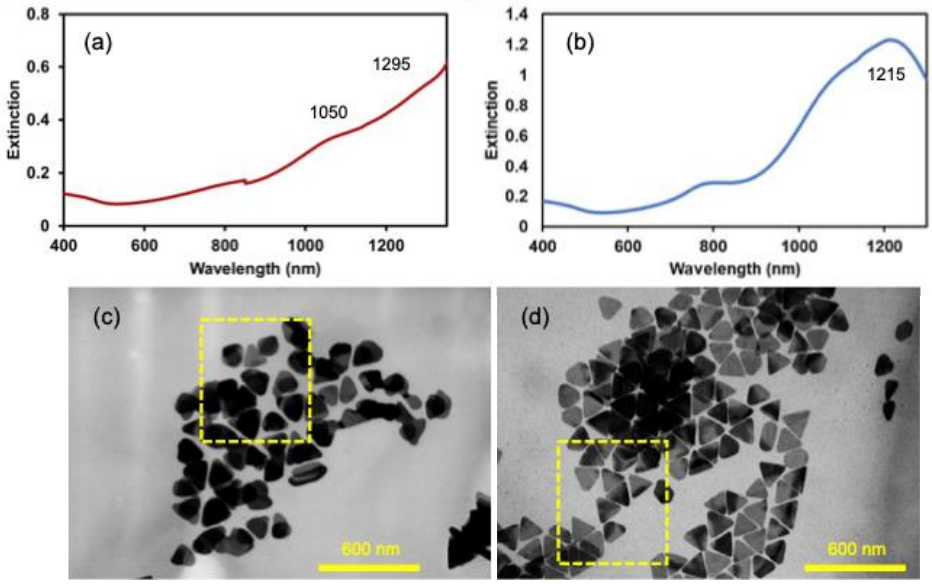


Figure 2. Characterization of AuNTs synthesized using different time intervals during seed addition. Extinction spectra of AuNTs prepared using (a) a longer and (b) a shorter time interval. STEM images of the corresponding samples: (c) longer time interval and (d) shorter time interval.

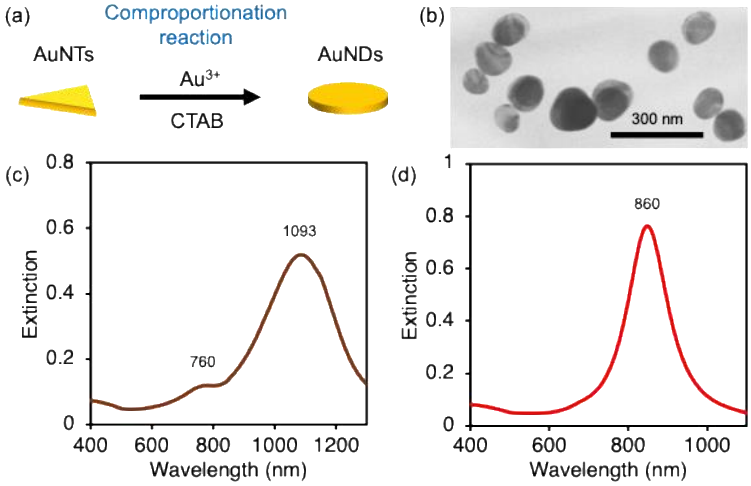


Figure 3. Transformation of AuNTs into AuNDs. (a) Schematic illustration of the comproportionation reaction. (b) STEM image of the resulting AuNDs. Extinction spectra of (c) AuNTs and (d) AuNDs.

This work is licensed under a Creative Commons Attribution-NonCommercial-ShareAlike 4.0 International License

The effect of seed-solution incubation time was further investigated. When the incubation time was reduced from 6 to 4 h, the resulting AuNTs exhibited a more clearly defined LSPR peak with a narrower full width at half maximum (FWHM; **Figure 3c**). This spectral change suggests a narrower distribution of optical responses under the shorter incubation condition. However, the extinction spectrum alone cannot establish the distribution of particle shapes. Therefore, the morphological observations should also be considered when evaluating the quality of the AuNTs. Variations in the extinction spectra were observed between synthesis batches prepared from the same seed solution. This observation suggests that the synthesis outcome was sensitive to the experimental procedure, particularly the timing of seed addition.[22] Extending the seed-addition duration beyond 5 s was associated with broader extinction peaks, indicating less uniform optical properties among the resulting particles. These findings highlight the importance of controlling the seed-addition procedure to improve the reproducibility of AuNT synthesis.

The AuNTs were subsequently converted into gold nanodiscs (AuNDs) through a comproportionation reaction involving Au^{3+} in the presence of CTAB (**Figure 3a**). In this process, the added gold precursor participates in the redox chemistry that drives morphological evolution of the initial nanoparticles. The proposed role of selective oxidation at surface sites with lower coordination numbers should be interpreted in accordance with the reaction mechanism reported in the literature.[22] Following the reaction, the extinction peak shifted from 1093 to 860 nm and became sharper (**Figure 3d**), indicating a substantial change in the optical response of the nanoparticles. This spectral change was consistent with the formation of AuNDs, as further supported by the STEM image (**Figure 3b**). The morphological assignment should primarily be based on the microscopy observations, while the extinction spectrum provides complementary evidence of the structural transformation. The LSPR response of AuNDs is sensitive to their dimensions, particularly their diameter and thickness, as previously reported.[23] Nevertheless, previous studies have reported analogous assembly and disassembly behavior for AuNDs with different diameters.[12] Based on these findings, the present study focuses on investigating the effects of alkyne and azide ligands on the thermoresponsive assembly behavior of AuNDs. This comparison provides insight into how differences in the terminal functional groups of the surface ligands may influence the assembly behavior of the nanoparticles.

b. Surface Modification of Gold Nanodiscs and Investigation of Assembly Properties

Initially, AuNDs were functionalized with a thermoresponsive ligand (**C1**) and a carboxylic acid-terminated ligand (**COOH**) via ligand exchange, followed by the determination of their assembly (T_A) and disassembly (T_D) temperatures according to the previously reported procedure[12] (**Table 1**). The **COOH** ligand was introduced to improve colloidal dispersibility by providing negatively charged carboxylate groups under basic conditions. At pH 8.0, partial or substantial deprotonation of the carboxylic acid groups may contribute to electrostatic repulsion between particles, potentially facilitating disassembly. The initial ligand composition consisted of 97% **C1** and 3% **COOH**, denoted as AuNDs-(97:3). Following ligand modification, the zeta potential shifted from +55.6 mV for CTAB-stabilized AuNDs to −13 mV for AuNDs-(97:3), indicating a change in the surface electrokinetic properties consistent with the introduction of anionic surface groups. Upon heating, the extinction intensity began to decrease at approximately 35 °C (**Figure 4a**), suggesting a temperature-dependent change in the colloidal state and the onset of particle association. Further heating to 70 °C resulted in a more pronounced decrease in extinction intensity, which may be associated with the formation of larger aggregates and subsequent sedimentation.

This work is licensed under a Creative Commons Attribution-NonCommercial-ShareAlike 4.0 International License

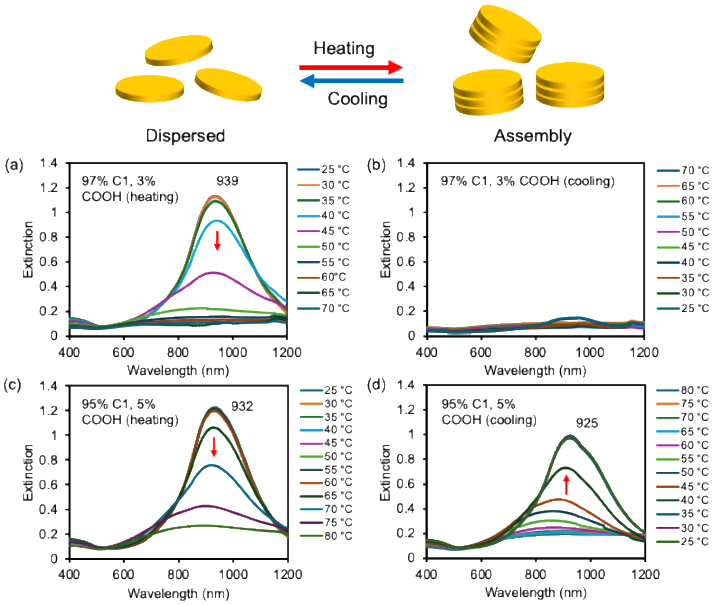


Figure 4. Extinction spectra of (a, b) AuNDs-(97:3) in 10 mM HEPES buffer (pH 8.0) during (a) heating from 25 to 70 °C and (b) cooling from 70 to 25 °C, and (c, d) AuNDs-(95:5) in the same buffer during (c) heating from 25 to 80 °C and (d) cooling from 80 to 25 °C.

Table 1. The assembly (T_A) and disassembly (T_D) temperatures of AuNDs modified with ligands.

Sample	Assembly Temperature (T_A)	Disassembly Temperature (T_D)
AuNDs-(97:3)	44 °C	Note determined
AuNDs-(97:5)	70 °C	44.8 °C
AuNDs-Alk-(90:5:5)	73.7 °C	42.2 °C
AuNDs-N3-(90:5:5)	45 °C	Note determined
AuNDs-Alk-(93:5:2)	65.9 °C	48.2 °C
AuNDs-N3-(93:5:2)	62.4 °C	45.4 °C

Upon cooling from 70 to 25 °C, the extinction spectrum of AuNDs-(97:3) did not recover to its initial state (**Figure 4b**). This incomplete spectral recovery indicates that the temperature-induced changes were not fully reversible under the conditions investigated. The result suggests that 3% **COOH** was insufficient to achieve complete recovery of the initial colloidal state, although the contribution of electrostatic repulsion cannot be isolated from other factors influencing particle interactions. To investigate the effect of **COOH** content, its proportion was increased to 5%, yielding AuNDs-(95:5). This sample exhibited temperature-dependent spectral changes during both heating and cooling (**Figures 4c** and **4d**), with greater recovery of the initial extinction spectrum after cooling. The onset of the spectral changes associated with assembly occurred at a higher temperature than that observed for AuNDs-(97:3). The zeta potential also shifted from -13 to -15 mV following the increase in **COOH** content. These observations suggest that changing the ligand composition influences the thermoresponsive behavior of AuNDs. However, the relatively small difference in zeta potential does not, by itself, establish that stronger electrostatic repulsion is the sole reason for the higher assembly temperature.

Subsequently, 5% of the **C1** ligand was replaced with either an alkyne-terminated ligand (**Alk**) or an azide-terminated ligand (**N3**), while maintaining the **COOH** content at 5%. The resulting samples were designated as AuNDs-**Alk**-(90:5:5) and AuNDs-**N3**-(90:5:5), respectively. Before heating, the extinction intensity of AuNDs-**N3**-(90:5:5) was approximately half that of AuNDs-**Alk**-(90:5:5)

This work is licensed under a Creative Commons Attribution-NonCommercial-ShareAlike 4.0 International License

at 25 °C (**Figures 5a** and **5c**). This difference suggests that the two samples had different initial optical responses and may reflect differences in their colloidal states. Nevertheless, extinction intensity alone cannot establish the relative degree of dispersion because it may also depend on particle concentration, scattering, aggregation, and sedimentation. Previous reports have described aggregation and limited colloidal stability in azide-functionalized AuNP systems in buffer solutions.[24,25] These findings provide relevant context, although differences in particle geometry, ligand structure, and experimental conditions should be considered when comparing those systems with the present AuNDs.

The incorporation of **Alk** or **N3** also altered the temperature-dependent spectral responses. Compared with AuNDs-(95:5), which exhibited an apparent assembly temperature of 70 °C, AuNDs-**Alk**-(90:5:5) showed the onset of assembly-associated spectral changes at approximately 73.7 °C during heating (**Table 1**). In contrast, AuNDs-**N3**-(90:5:5) exhibited T_A at approximately 45°C. Thus, the observed assembly temperatures differed substantially between the **Alk**- and **N3**-modified samples. This difference indicates that the identity of the incorporated ligand is associated with the temperature at which the spectral response occurs. However, the underlying mechanism cannot be assigned exclusively to ligand hydrophobicity because the initial colloidal states and other ligand-dependent interparticle interactions may also contribute

During cooling from 80 to 25 °C, the extinction spectrum of AuNDs-**Alk**-(90:5:5) nearly recovered to its initial state, with the apparent disassembly transition occurring between 40 and 45 °C (**Figure 5b**). In contrast, AuNDs-**N3**-(90:5:5) did not recover its initial extinction spectrum after cooling to 25 °C (**Figure 5d**). This result indicates that the temperature-dependent spectral changes in the N3-containing sample are incompletely reversible under the conditions examined. The incomplete recovery may reflect persistent particle association or other changes in the colloidal state. Although differences in hydrophobic interactions or interparticle interactions could contribute, the present measurements do not establish a specific molecular mechanism, such as enhanced hydrogen bonding, for the observed behavior. Therefore, the **N3** content was subsequently reduced to investigate whether a lower proportion of this ligand would improve the reversibility of the temperature-dependent response.

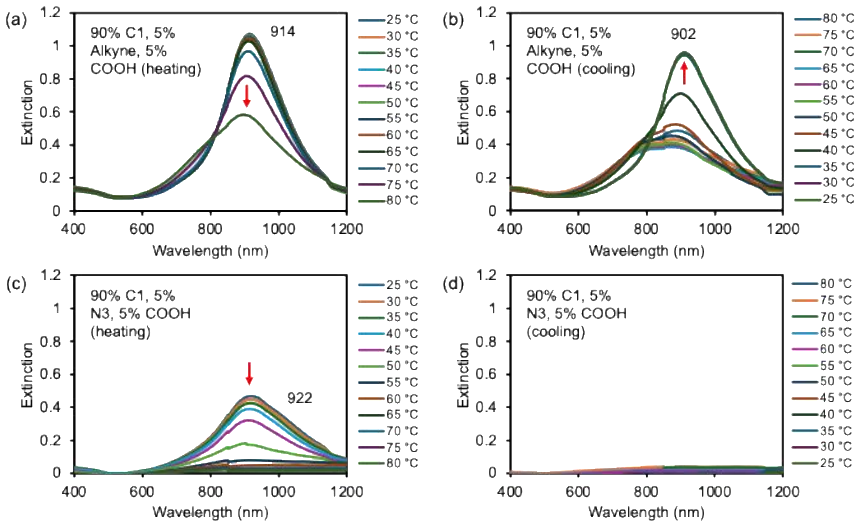


Figure 5. Extinction spectra of AuNDs modified with 5% **Alk** or **N3** ligand in 10 mM HEPES buffer (pH 8.0) during heating and cooling. (a, b) AuNDs-**Alk**-(90:5:5) during (a) heating from 25 to 80 °C and (b) cooling from 80 to 25 °C. (c, d) AuNDs-**N3**-(90:5:5) during (c) heating from 25 to 80 °C and (d) cooling from 80 to 25 °C.

This work is licensed under a Creative Commons Attribution-NonCommercial-ShareAlike 4.0 International License

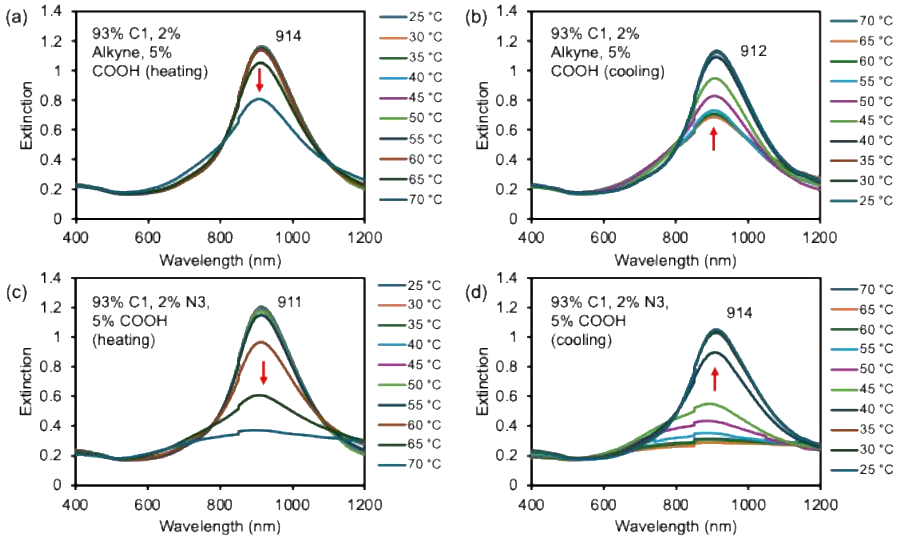


Figure 6. Extinction spectra of AuNDs modified with 2% **Alk** or **N3** ligand in 10 mM HEPES buffer (pH 8.0). (a, b) AuNDs-**Alk**-(93:5:2) during (a) heating from 25 to 80 °C and (b) cooling from 80 to 25 °C. (c, d) AuNDs-**N3**-(93:5:2) during (c) heating from 25 to 80 °C and (d) cooling from 80 to 25 °C.

The **Alk** and **N3** contents were then reduced from 5% to 2%, while the **COOH** content was maintained at 5%. The resulting samples were designated as AuNDs-**Alk**-(93:5:2) and AuNDs-**N3**-(93:5:2), respectively. For AuNDs-**Alk**-(93:5:2), the apparent assembly temperature decreased to 65.9 °C, whereas the apparent disassembly temperature increased to 48.2 °C (**Table 1**). Compared with the corresponding 5% **Alk** sample, these changes indicate a narrower temperature interval between the observed assembly and disassembly transitions. This behavior suggests that the proportion of **Alk** in the ligand mixture influences the temperature-dependent response and its apparent reversibility.

For AuNDs-**N3**-(93:5:2), reducing the **N3** content shifted the apparent assembly temperature to a higher range than that observed for AuNDs-**N3**-(90:5:5) (**Figures 5c** and **6c**). The extinction intensity at 25 °C before heating was also higher for the sample containing 2% **N3**, suggesting a difference in its initial optical or colloidal state. During cooling from 70 to 25 °C, AuNDs-**N3**-(93:5:2) exhibited temperature-dependent spectral changes consistent with substantial disassembly (**Figure 6d**), indicating improved reversibility compared with the corresponding sample containing 5% **N3**. These findings demonstrate that reducing the **N3** content was associated with changes in both the initial extinction response and the reversibility of the temperature-dependent behavior.

Overall, the extinction spectra reveal that the temperature-dependent assembly and disassembly behavior of AuNDs varies with ligand composition and the proportion of the incorporated functional ligands. The differences observed between the **Alk**- and **N3**-containing samples, together with the changes resulting from reducing their respective ligand contents, highlight the importance of surface composition in determining the observed thermoresponsive response. Nevertheless, because the present analysis is based primarily on extinction spectra, the proposed relationships between ligand composition, hydrophobicity, interparticle interactions, and colloidal stability should be regarded as interpretations rather than direct demonstrations of the underlying mechanisms. Further characterization would be required to distinguish changes in particle association from aggregation, sedimentation, and other contributions to the measured optical response. A limitation of this study is that, although the synthesis of AuNDs and subsequent ligand modification were repeated, the thermoresponsive assembly and disassembly behavior was not evaluated using samples from independent synthesis batches. Consequently,

This work is licensed under a Creative Commons Attribution-NonCommercial-ShareAlike 4.0 International License

batch-to-batch variability in the observed temperature-dependent responses could not be assessed. Future studies should evaluate the thermoresponsive behavior of independently prepared batches to assess reproducibility and quantify associated experimental variability.

Conclusion

AuNDs were successfully modified with thermoresponsive (**C1**) and negatively charged (**COOH**)-terminated ligands through a ligand exchange reaction. The resulting AuNDs exhibited reversible assembly and disassembly upon heating and cooling, demonstrating the thermoresponsive behavior of the mixed ligand system. Incorporation of 5% **Alk** or 5% **N3** ligands significantly altered the assembly temperature and reversibility of the thermal response. **N3**-containing AuNDs exhibited aggregation at lower temperatures and did not recover their initial extinction spectra upon cooling, whereas **Alk**-containing AuNDs showed aggregation at higher temperatures and substantial spectral recovery during cooling. These differences may be associated with variations in ligand-mediated interparticle interactions, hydration, and surface packing, although the underlying mechanisms require further investigation. Reducing the **Alk** or **N3** content to 2% enabled the recovery of reversible assembly and disassembly behavior under the investigated conditions. Overall, these findings demonstrate that the composition of the surface-bound ligands plays an important role in controlling the thermal assembly properties and reversibility of AuNDs. Future studies will explore the use of copper(I)-catalyzed azide–alkyne cycloaddition (CuAAC) to covalently connect **Alk**- and **N3**-functionalized AuNDs, aiming to construct more stable and structurally controlled assemblies.

References

1. Jana J, Ganguly M, Pal T. Enlightening surface plasmon resonance effect of metal nanoparticles for practical spectroscopic application. RSC Adv 2016;6:86174–211. https://doi.org/10.1039/C6RA14173K.
2. Mayer KM, Hafner JH. Localized Surface Plasmon Resonance Sensors. Chem Rev 2011;111:3828–57. https://doi.org/10.1021/cr100313v.
3. Ghosh SK, Pal T. Interparticle Coupling Effect on the Surface Plasmon Resonance of Gold Nanoparticles: From Theory to Applications. Chem Rev 2007;107:4797–862. https://doi.org/10.1021/cr0680282.
4. Roy S, Kashyap RK, Pillai PP. Thermoplasmonics Enable the Coupling of Light into the Solvent-Mediated Self-Assembly of Gold Nanoparticles. The Journal of Physical Chemistry C 2023;127:10355–65. https://doi.org/10.1021/acs.jpcc.3c01316.
5. Willets KA, Van Duyne RP. Localized Surface Plasmon Resonance Spectroscopy and Sensing. Annu Rev Phys Chem 2007;58:267–97. https://doi.org/10.1146/annurev.physchem.58.032806.104607.
6. Amendola V, Pilot R, Frasconi M, Maragò OM, Iatì MA. Surface plasmon resonance in gold nanoparticles: a review. Journal of Physics: Condensed Matter 2017;29:203002. https://doi.org/10.1088/1361-648X/aa60f3.
7. Kelly KL, Coronado E, Zhao LL, Schatz GC. The Optical Properties of Metal Nanoparticles: The Influence of Size, Shape, and Dielectric Environment. J Phys Chem B 2003;107:668–77. https://doi.org/10.1021/jp026731y.
8. Zorić I, Zäch M, Kasemo B, Langhammer C. Gold, Platinum, and Aluminum Nanodisk Plasmons: Material Independence, Subradiance, and Damping Mechanisms. ACS Nano 2011;5:2535–46. https://doi.org/10.1021/nn102166t.
9. Boles MA, Engel M, Talapin D V. Self-Assembly of Colloidal Nanocrystals: From Intricate Structures to Functional Materials. Chem Rev

This work is licensed under a Creative Commons Attribution-NonCommercial-ShareAlike 4.0 International License

2016;116:11220–89. https://doi.org/10.1021/acs.chemrev.6b00196.

10. O'Dwyer C, Gay G, Viaris de Lesegno B, Weiner J. The Nature of Alkanethiol Self-Assembled Monolayer Adsorption on Sputtered Gold Substrates. Langmuir 2004;20:8172–82. https://doi.org/10.1021/la049103b.
11. Xiong K, Nagayama M, Ijiro K, Mitomo H. Fair surface modification with mixed alkanethiols on gold nanoparticles through minimal unfair ligand exchange. Nanoscale Adv 2024;6:4583–90. https://doi.org/10.1039/D4NA00270A.
12. Mba JC, Mitomo H, Yonamine Y, Wang G, Matsuo Y, Ijiro K. Hysteresis in the Thermo-Responsive Assembly of Hexa(ethylene glycol) Derivative-Modified Gold Nanodiscs as an Effect of Shape. Nanomaterials 2022;12:1421. https://doi.org/10.3390/nano12091421.
13. Iida R, Mitomo H, Niikura K, Matsuo Y, Ijiro K. Two-Step Assembly of Thermoresponsive Gold Nanorods Coated with a Single Kind of Ligand. Small 2018;14. https://doi.org/10.1002/smll.201704230.
14. Xiong K, Mitomo H, Su X, Shi Y, Yonamine Y, Sato S, et al. Molecular configuration-mediated thermo-responsiveness in oligo(ethylene glycol) derivatives attached on gold nanoparticles. Nanoscale Adv 2021;3:3762–9. https://doi.org/10.1039/D1NA00187F.
15. Iida R, Mitomo H, Matsuo Y, Niikura K, Ijiro K. Thermoresponsive Assembly of Gold Nanoparticles Coated with Oligo(Ethylene Glycol) Ligands with an Alkyl Head. The Journal of Physical Chemistry C 2016;120:15846–54. https://doi.org/10.1021/acs.jpcc.5b11687.
16. Chen C, Lin Z, Lin F, Huang L, Lin C, Huang J. Using click reaction to covalently link heterogeneous gold nanorods into head-to-head one-dimensional chains with an alternating sequence as plasmonic Fano resonators. Journal of the Chinese Chemical Society 2023;70:1399–408. https://doi.org/10.1002/jccs.202300048.
17. Tian T, Yang W, Wang X, Liu T, Pan B, Guo W, et al. Click chemistry-enabled gold nanorods for sensitive detection and viability evaluation of copper(II)-reducing bacteria. Mater Today Bio 2025;30:101453. https://doi.org/10.1016/j.mtbio.2025.101453.
18. Baradaran Kayyal T, Kizhake Veetil V, Mathew R, Ajiboye L, Lowrance CM, Guzman J, et al. Directed Assembly of Gold Bipyramids and Quantum Dots Using Click Chemistry for Plasmon-Exciton Coupling. ACS Appl Nano Mater 2025;8:18751–61. https://doi.org/10.1021/acsanm.5c02896.
19. Bui H-TD, Park Y, Jung YM, Chew SY, Yoo HS. Reactive oxygen species-responsive clicked assembly of gold nanoparticles to enhance photothermal therapy. J Mater Chem B 2023;11:6961–74. https://doi.org/10.1039/D3TB00500C.
20. Sun Z, Umar A, Zeng J, Luo X, Song L, Zhang Z, et al. Highly Pure Gold Nanotriangles with almost 100% Yield for Surface-Enhanced Raman Scattering. ACS Appl Nano Mater 2022;5:1220–31. https://doi.org/10.1021/acsanm.1c03827.
21. Huang Y, Ferhan AR, Gao Y, Dandapat A, Kim D-H. High-yield synthesis of triangular gold nanoplates with improved shape uniformity, tunable edge length and thickness. Nanoscale 2014;6:6496–500. https://doi.org/10.1039/C4NR00834K.
22. O'Brien MN, Jones MR, Kohlstedt KL, Schatz GC, Mirkin CA. Uniform Circular Disks With Synthetically

This work is licensed under a Creative Commons Attribution-NonCommercial-ShareAlike 4.0 International License

Tailorable Diameters: Two-Dimensional Nanoparticles for Plasmonics. Nano Lett 2015;15:1012–7. https://doi.org/10.1021/nl5038566.

23. Hassan NA, Hashim AM. The effect of size of Au nanodisc on the localized surface plasmon resonance simulated using finite-difference time-domain (FDTD) method. Mater Today Proc 2019;7:607–11. https://doi.org/10.1016/j.matpr.2018.12.014.
24. Li N, Binder WH. Click-chemistry for nanoparticle-modification. J Mater Chem 2011;21:16717. https://doi.org/10.1039/c1jm11558h.
25. Brennan JL, Hatzakis NS, Tshikhudo TR, Nijole Dirvianskyte, Razumas V, Patkar S, et al. Bionanoconjugation via Click Chemistry: The Creation of Functional Hybrids of Lipases and Gold Nanoparticles. Bioconjug Chem 2006;17:1373–5. https://doi.org/10.1021/bc0601018.

This work is licensed under a Creative Commons Attribution-NonCommercial-ShareAlike 4.0 International License